Supplemental material

Semi-Continuous Measurements of Gas/Particle Partitioning of Organic Acids in a Ponderosa Pine Forest Using a MOVI-HRToF-CIMS

Reddy L. N. Yatavelli,[1,2,3] Harald Stark,[2,4] Samantha L. Thompson,[1,2] Joel R. Kimmel,[3,5] Michael J. Cubison,[5] Douglas A. Day,[1,2] Pedro Campuzano-Jost,[1,2] Brett B. Palm,[1,2] Alma Hodzic,[6] Joel A. Thornton,[7] John T. Jayne,[4] Douglas R. Worsnop,[4,8] Jose L. Jimenez[1,2,*]

[1] Cooperative Institute for Research in Environmental Sciences, University of Colorado, Boulder, CO, 80309 USA

[2] Department of Chemistry and Biochemistry, University of Colorado, Boulder, CO, 80309 USA

[3] Division of Atmospheric Sciences, Desert Research Institute, Reno, NV, 89512 USA

[4] Aerodyne Research Inc., Billerica, MA, 01821 USA

[5] TOFWERK AG., 3600 Thun, Switzerland

[6] National Center for Atmospheric Research, Boulder, CO, 80301 USA

[7] Department of Atmospheric Sciences, University of Washington, Seattle, WA, 98105 USA

[8] Department of Physics, University of Helsinki, Helsinki 00014, Finland

* To whom correspondence should be addressed: jose.jimenez@colorado.edu

1. MOVI Cycle

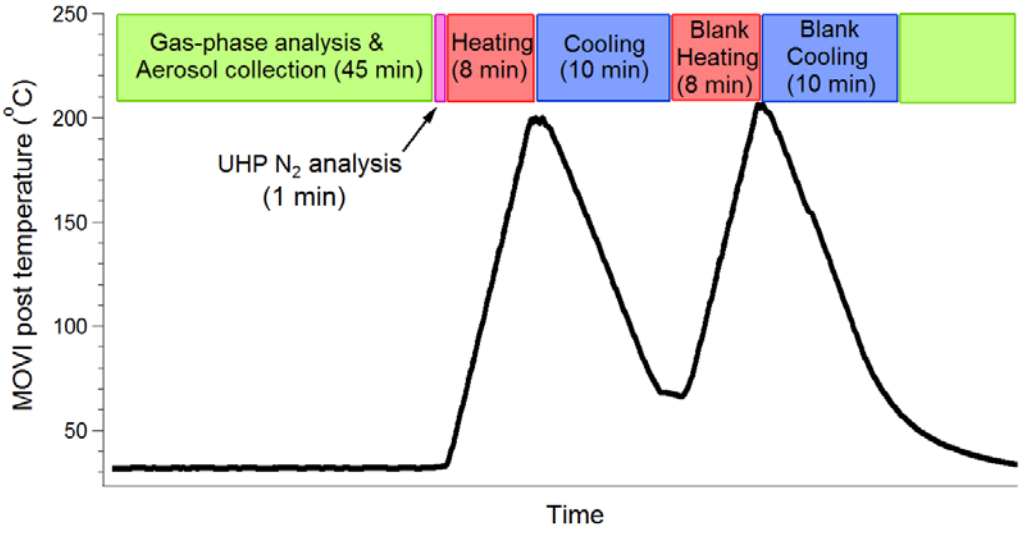

Figure S1. MOVI steps during BEACHON-RoMBAS field study

2. High-Resolution Peak Fitting of 183 Th

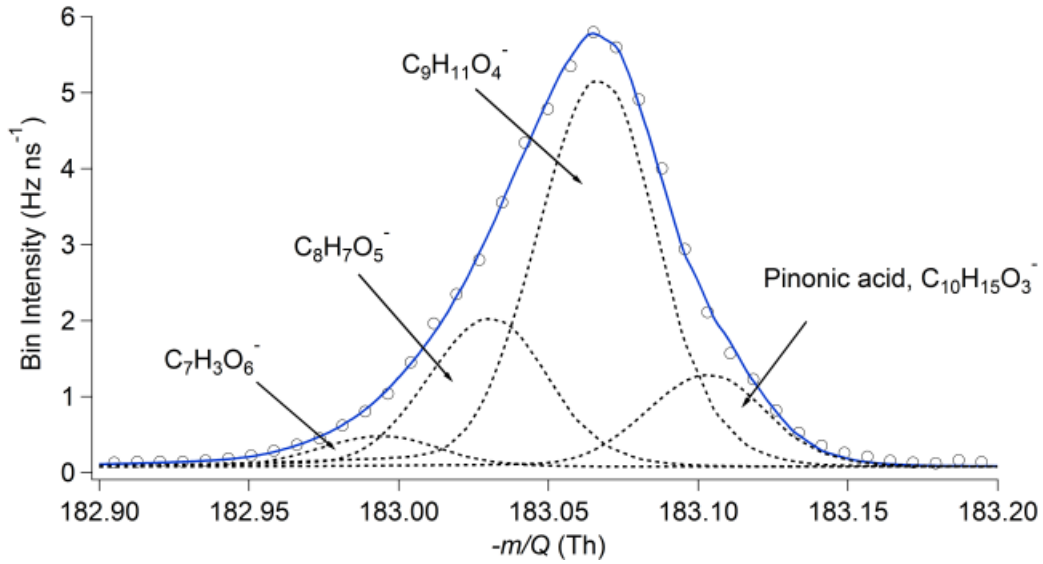

Figure S2. High resolution multi peak fitting result of 183 Th showing several different isobaric compounds.

3. Alkanoic acid signals on August 26, 2011

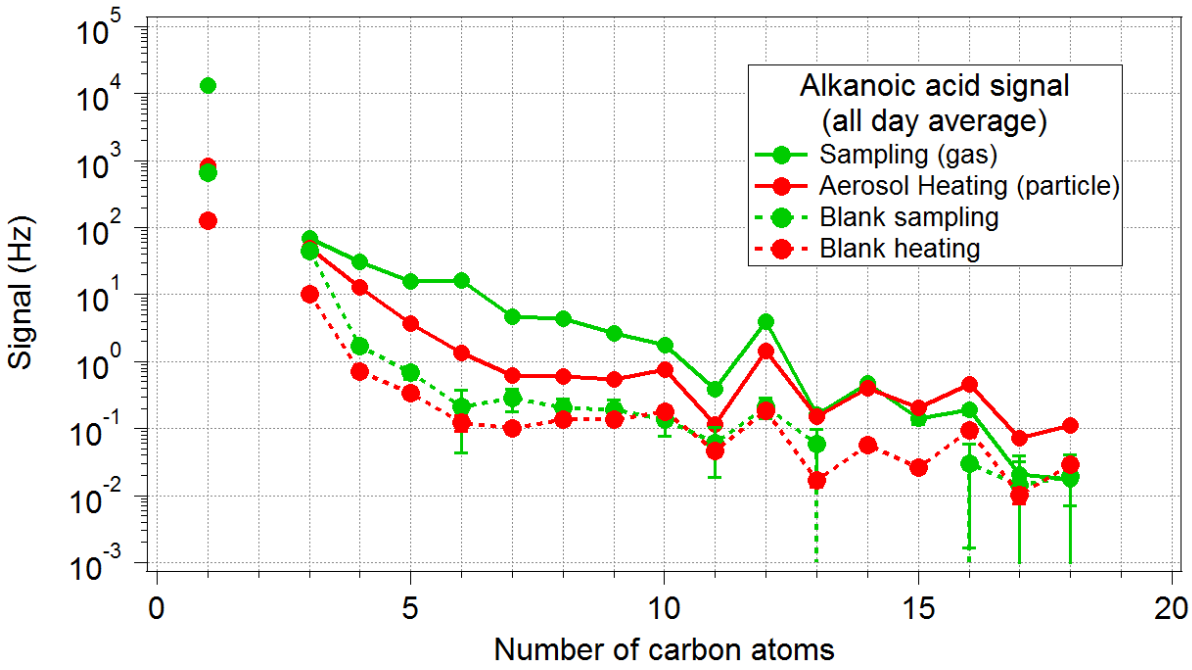

Figure S3. All-day average signals measured at each alkanoic acid during *Sampling* (gas), *Aerosol Heating* (particle), *Blank Sampling* and *Blank Heating* steps. Signals are from August 26, 2011.

4. Estimated partitioning of alkanoic acids to the aerosol aqueous phase

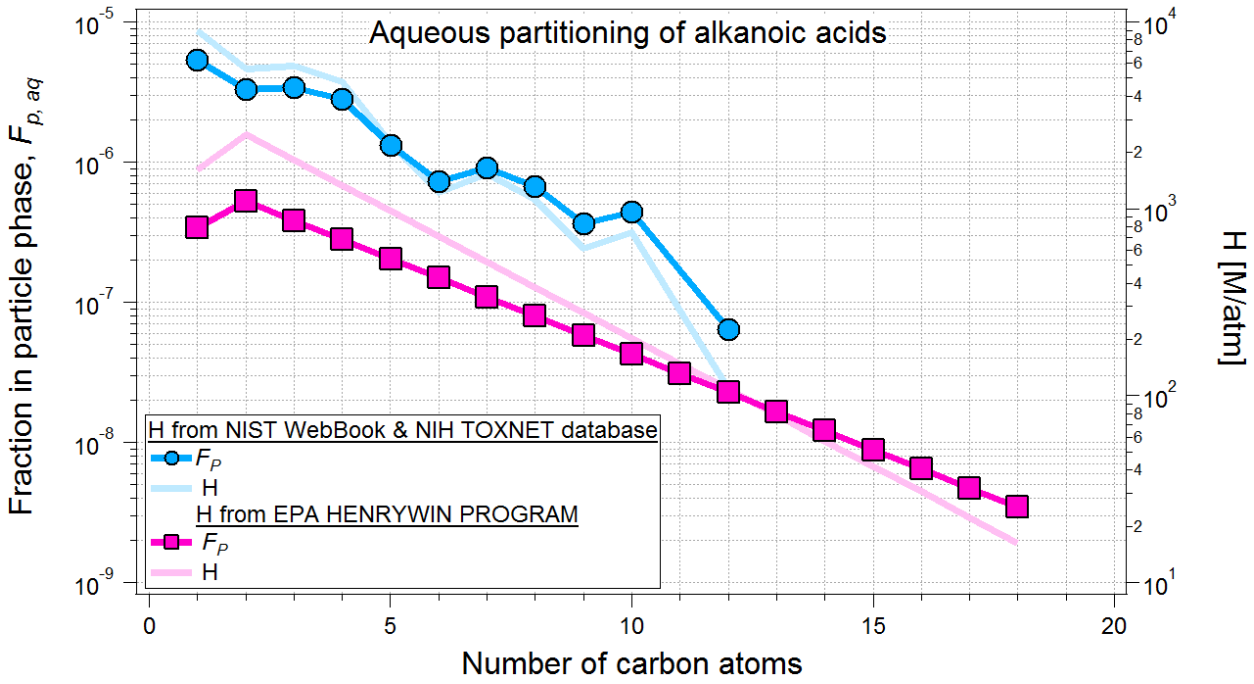

Figure S4. Calculated partitioning to aerosol aqueous phase using Henry's law coefficients from different sources. Aerosol LWC is calculated using the E-AIM II (Clegg et al., 1998; E-AIM, 2012). Aerosol ionic composition as measured by the AMS. Highest RH was fixed at 99% for the LWC calculations. Henry's law constants (H) for C_1-C_{12} alkanoic acids are from NIST Chemistry WebBook (Sander, 2011), and National Institutes of Health TOXNET database (ChemIDplus, 1986), and for C_1-C_{18} are from the US EPA HENRYWIN program (EPA, 2013).

5. Relative humidity and ambient temperature from Aug 20 – 30, 2011

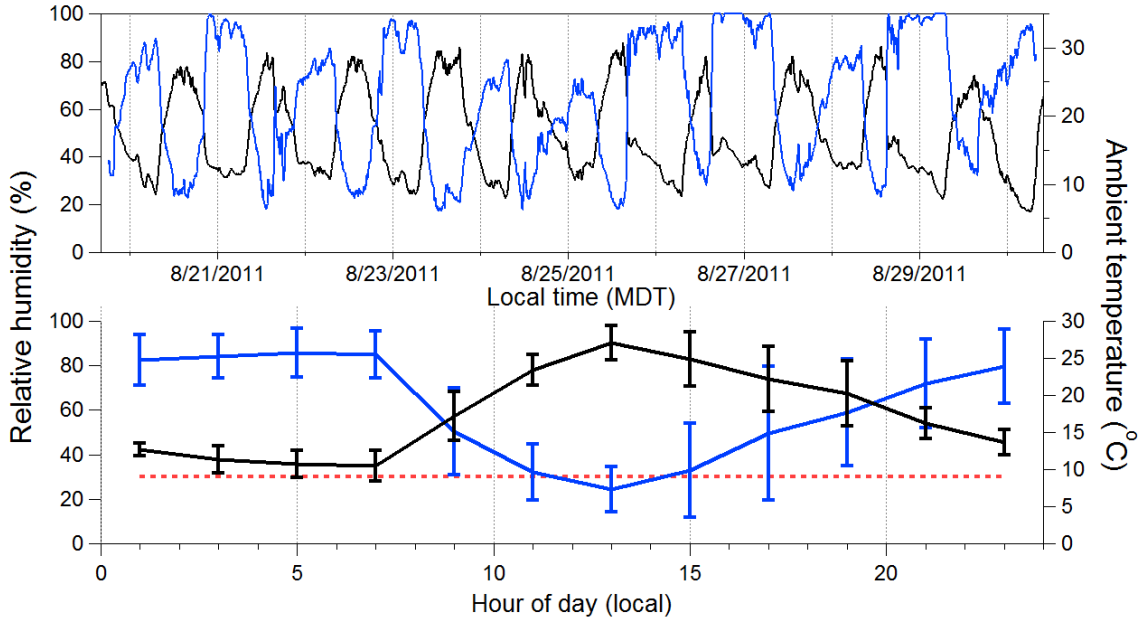

Figure S5. Relative humidity and ambient temperature during the measurement period. Dotted red line indicated RH = 30%. Error bars in the diurnal cycle represent day-to-day variability.

6. *Sampling* and *Aerosol Heating* signals in the C_{12} bin on August 26, 2011

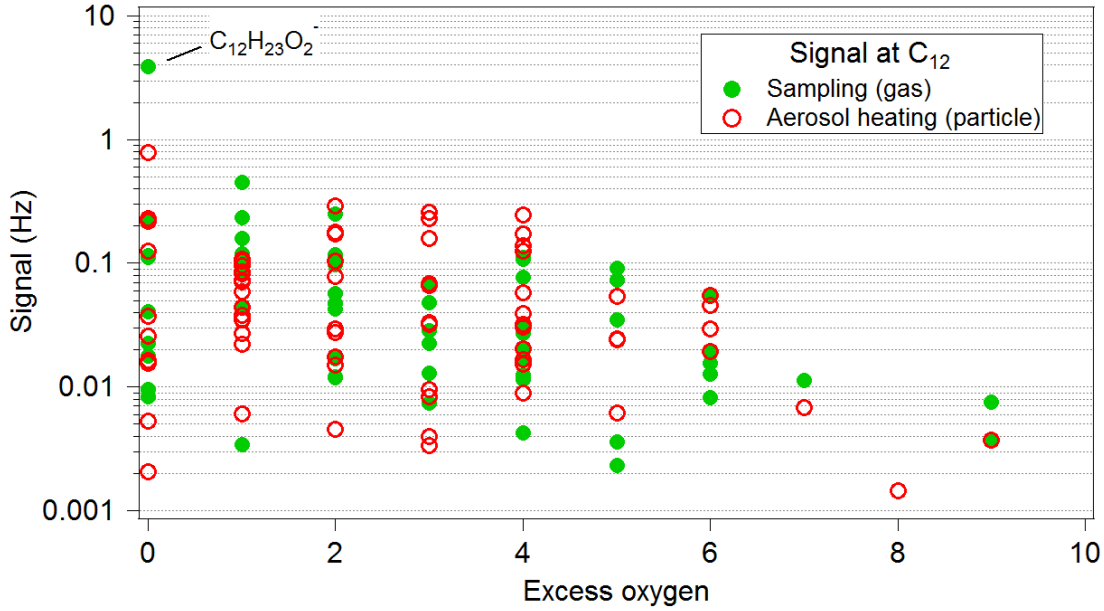

Figure S6. All day averaged *Sampling* and *Aerosol Heating* signals measured for various ions with 12 carbons.

7. Estimating H for bulk acids vs. carbon number:

Since experimental data for H of functionalized acids of different carbon numbers are not available, $F_{p,aq}$ of bulk acids is estimated using two different estimates: 1) from the H of pure mono and di-acids and the average excess oxygen at each carbon number; and 2) from the values estimated by Hodzic et al. (2013) for functionalized acids using group contribution theory. Di-acid H values are from EPA HENRYWIN program (EPA, 2013) and Compernolle and Müller (2013). Tables S3 lists the H values used in the $F_{p,aq}$ calculation here. For calculating H of bulk-averaged acids from mono and di-acids we calculated the geometric mean of mono and di-acid H values weighed by the measured excess O for a given carbon number (shown in Fig 5 of the main manuscript), since the excess O is always on average between 0 (value for monoacids) and 2 (value for diacids). The following equation is used:

$$\mathrm{H_{bulk,i}} = 10\text{^}([\log_{10}(\mathrm{abs}\left(\frac{[\mathrm{excessO_i} - 2]}{2}\right) * \mathrm{H_{mono}} + \log_{10}(\mathrm{abs}\left(\frac{[\mathrm{excessO_i}]}{2}\right) * \mathrm{H_{diacid}}]/2)$$

The values of H for bulk-averaged acid estimated from the group contribution theory-based estimates from Hodzic et al. (2013) are from 413 multifunctional acids. The H values are first binned into carbon number bins and further separated based on their excess O. A geometric mean is then calculated for only those acids having an excess O of 1 and 2 resulting in two H values for each carbon number, $H_{exO=1}$ and $H_{exO=2}$. This limitation of excess O = 2 is based on the fact that the measured excess O is < 2 for C_1-C_{18} carbon numbers (shown in Fig 5 of the main manuscript). Finally, a geometric mean of $H_{exO=1}$ and $H_{exO=2}$ is calculated and weighed by the measured excess O using the equation,

$$\mathrm{H_{bulk,i}} = 10\text{^}([\log_{10}(\mathrm{abs}([\mathrm{excessO_i} - 2]) * \mathrm{H_{exO=1,i}} + \log_{10}(\mathrm{abs}([\mathrm{excessO_i} - 1]) * \mathrm{H_{exO=2,i}}]/2)$$

All values of H are at 298 K. The geometric mean H values show a spread of 1-2 orders of magnitude for a given carbon number (Fig. S7 below). $F_{p,aq}$ is estimated using the aerosol liquid water content (LWC) content calculated with the E-AIM model-II. For LWC calculation highest RH is fixed at 99% since above this the model gave un-realistically high LWC, and if such values of RH > 99% were reached in the field the particles would grow beyond the size ranges of the instrumentation. Figure 6 in the main manuscript shows campaign average $F_{p,aq}$ for bulk-averaged acids as a function of carbon number using the datasets described above. The partitioning of bulk-averaged acids to the aqueous-phase is very small (below 0.5%) independent of the data source used for H. These values are lower than those calculated by partitioning to the organic fraction, and have the opposite trend with carbon number than observed experimentally.

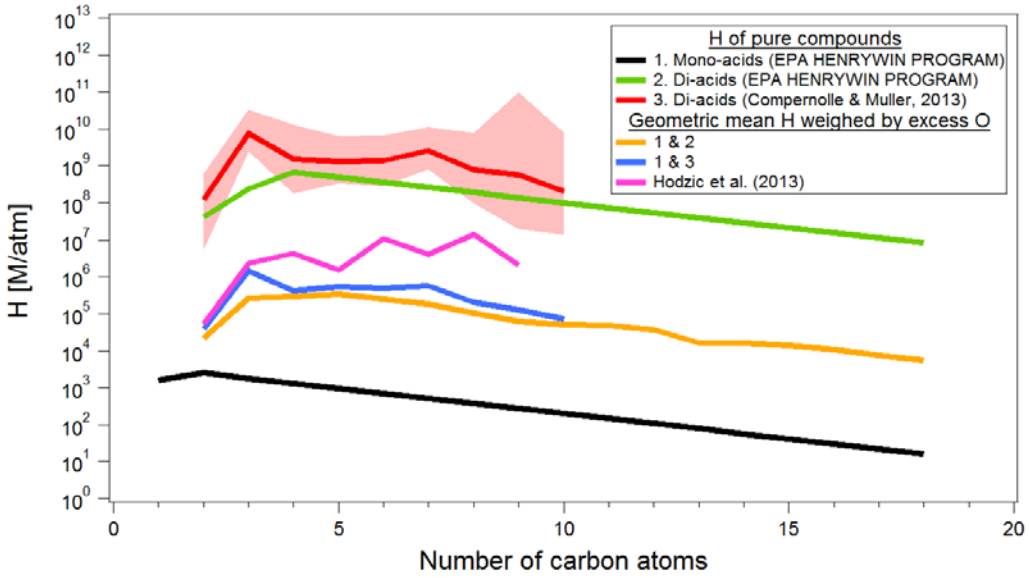

Figure S7. H values from various sources and the geometric mean estimated according to the description provided in section 7. The range of H values for Compernolle and Muller (2013) are the range reported in their manuscript for each carbon number.

8. Meteorology and OA on August 26, 2011

Fig. S8 shows the time series of ambient temperature, RH, OA, and photosynthetically-active radiation (PAR) on 26 Aug 2011. Temperature and RH varied between 8 – 29 ^{o}C and 24 – 100 %, respectively, with an average temperature of 15.8 ^{o}C. During brief rain showers from 3 – 5 PM (local time, UTC-6:00) temperature decreased by 10 - 15 ^{o}C and RH increased from 30 to 100 %. Total precipitation for this day was 7.1 mm. OA mass concentration did not show any clear diurnal pattern on this day (nor typically throughout the campaign) with an average OA mass concentration of 2.4 µg m^{-3}.

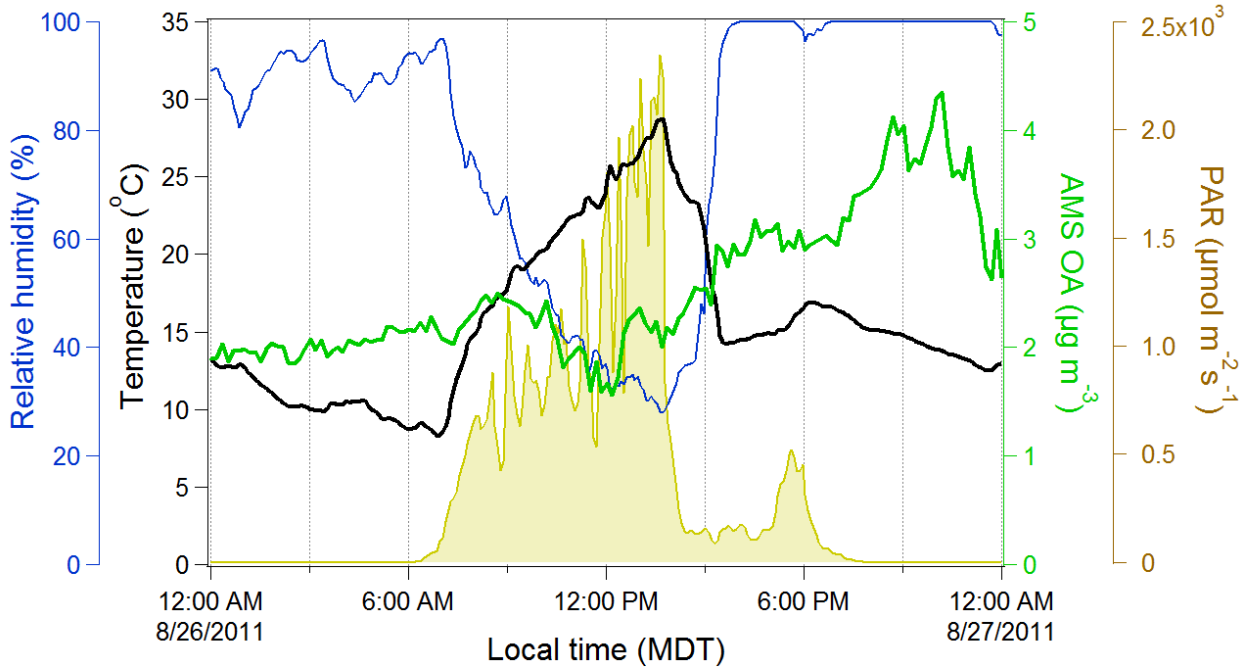

Figure S8. Time series of temperature, RH, OA and PAR on August 26, 2011. No precipitation was observed on this day.

9. Time series, diurnal average and scatter plot of measured and modeled F_p for bulk-averaged acids.

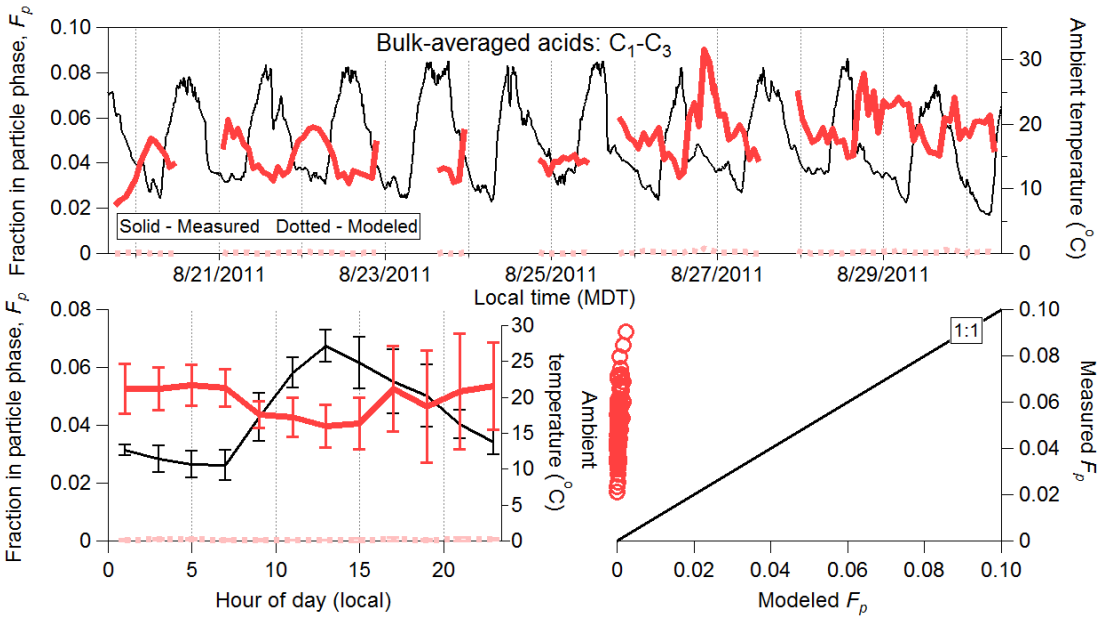

Figure S9. Time series, diurnal cycle and scatter plot of measured and modeled F_p for C_1-C_3 averaged bulk acids. Model uses excess oxygen as a hydroxyl group.

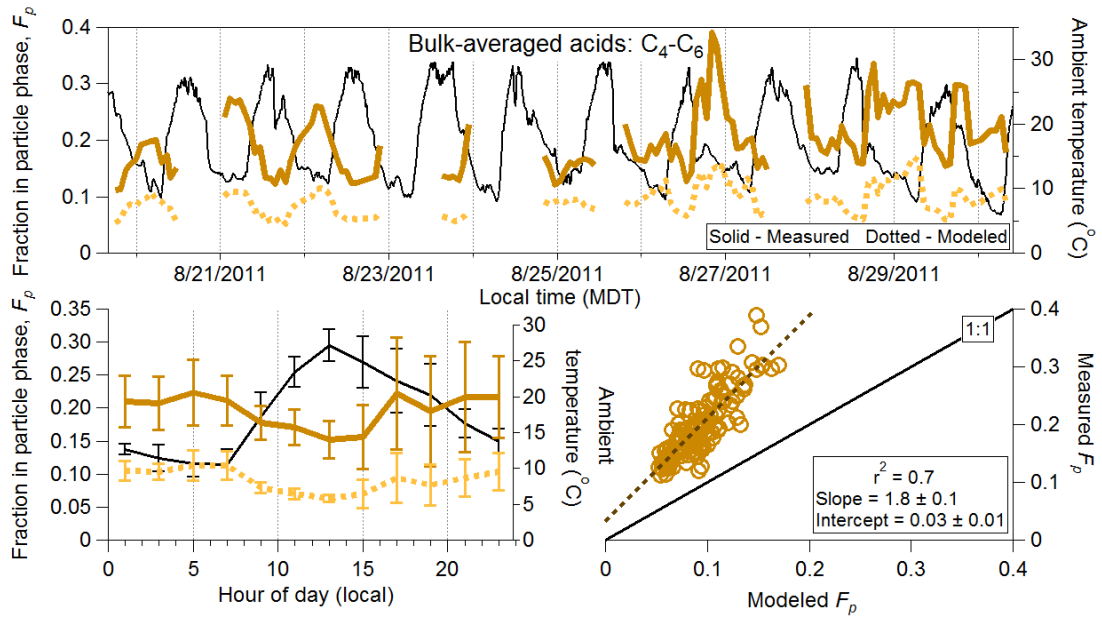

Figure S10. Time series, diurnal cycle and scatter plot of measured and modeled F_p for C_4-C_6 averaged bulk acids. Model uses excess oxygen as a hydroxyl group.

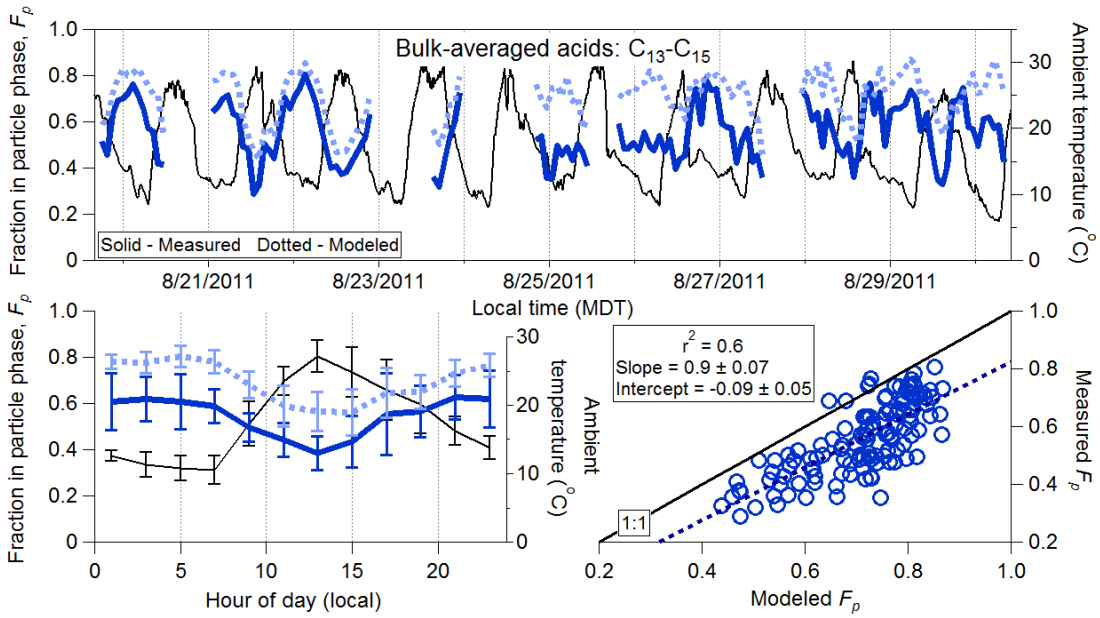

Figure S11. Time series, diurnal cycle and scatter plot of measured and modeled F_p for C_{13}-C_{15} averaged bulk acids. Model uses excess oxygen as a hydroxyl group.

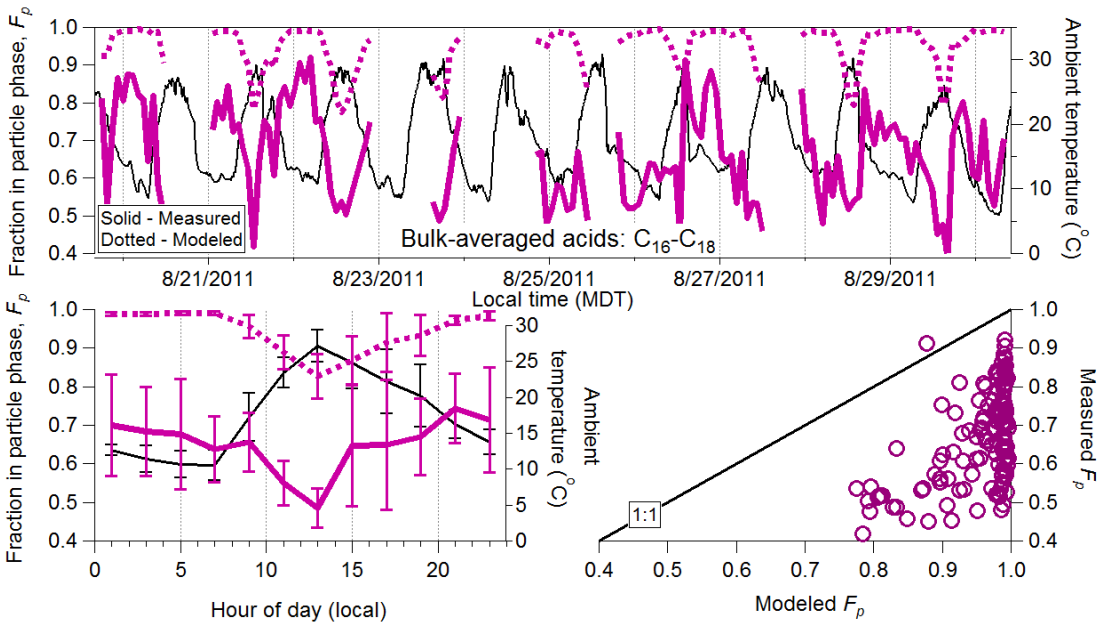

Figure S12. Time series, diurnal cycle and scatter plot of measured and modeled F_p for C_{16}-C_{18} averaged bulk acids. Model uses excess oxygen as a hydroxyl group.

10. Time series modeled $F_{p,aq}$ for bulk-averaged and terpenoic acids.

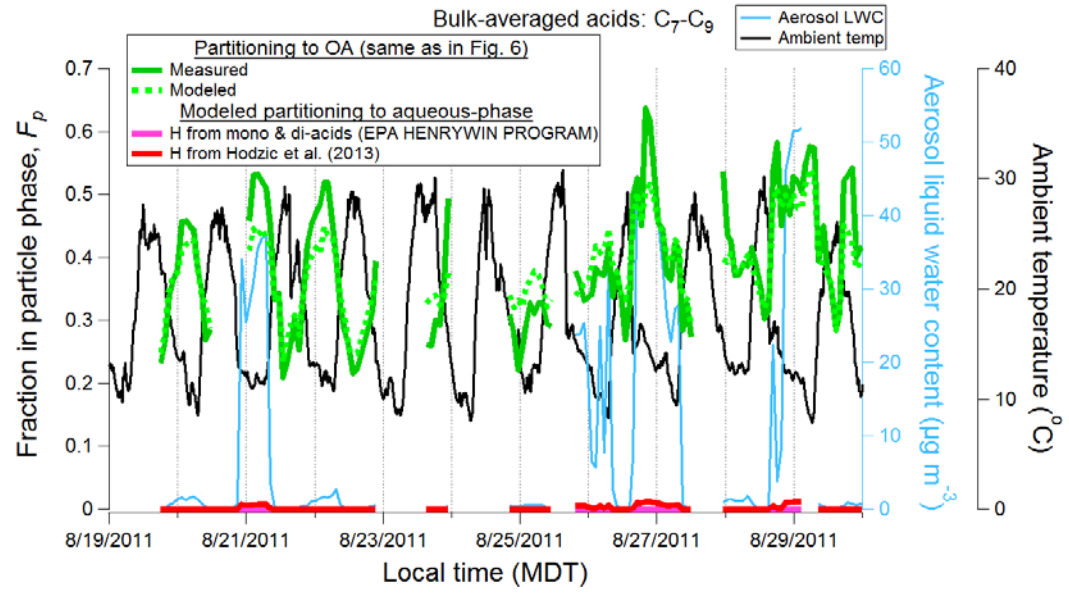

Figure S13. Time series of partitioning to organic and aqueous-phases for C_7-C_9 bulk acids. Also shown is the time series of ambient temperature and aerosol LWC calculated using the E-AIM model-II.

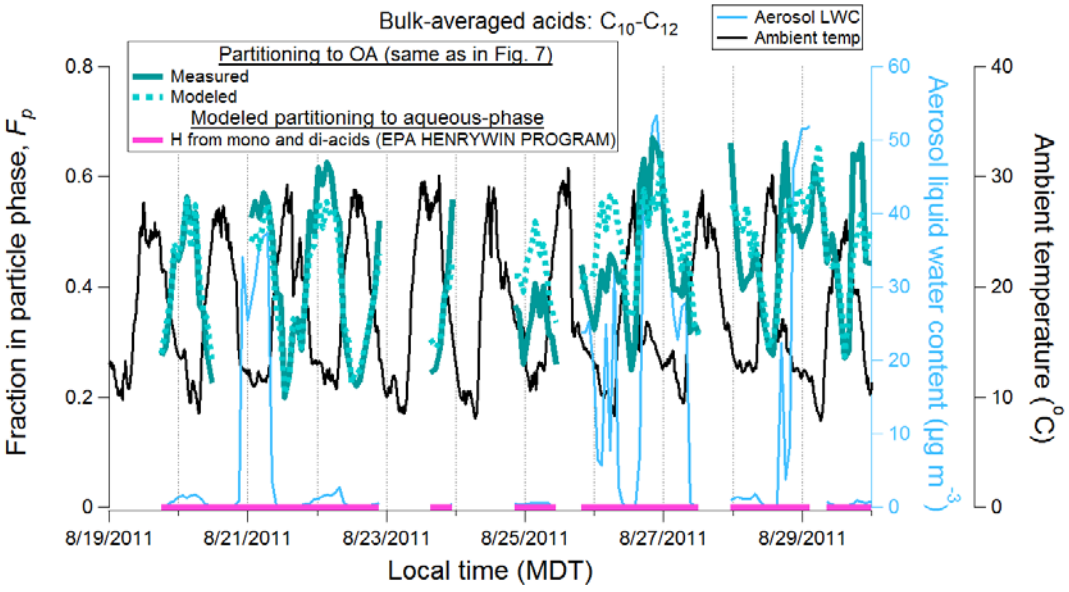

Figure S14. Time series of partitioning to organic and aqueous-phases for C_{10}-C_{12} bulk acids. Also shown is the time series of ambient temperature and aerosol LWC calculated using the E-AIM model-II.

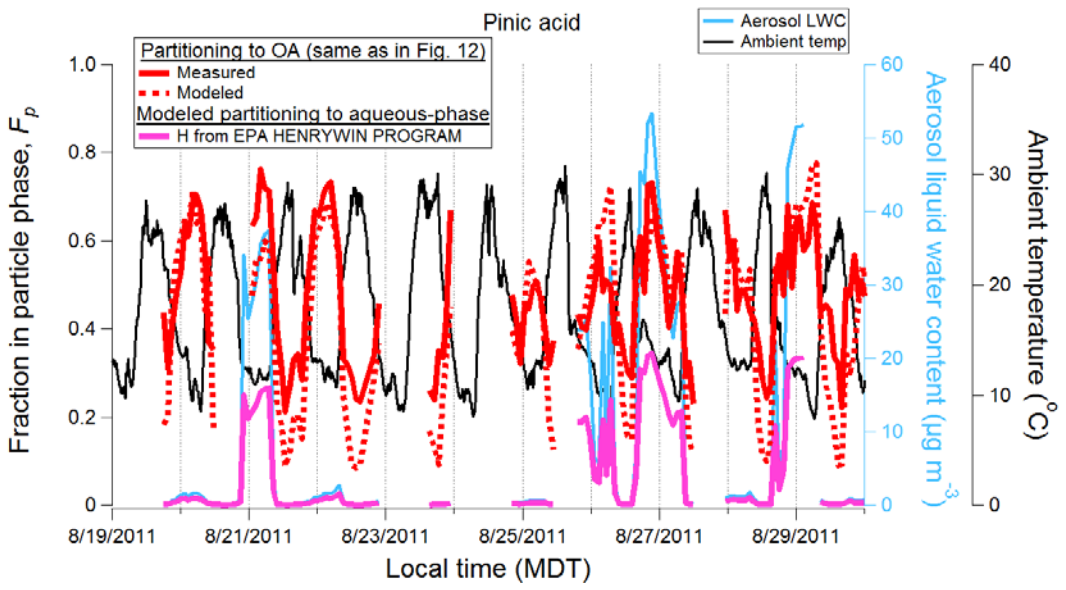

Figure S15. Time series of partitioning to organic and aqueous-phases for pinic acid. Also shown is the time series of ambient temperature and aerosol LWC calculated using the E-AIM model-II.

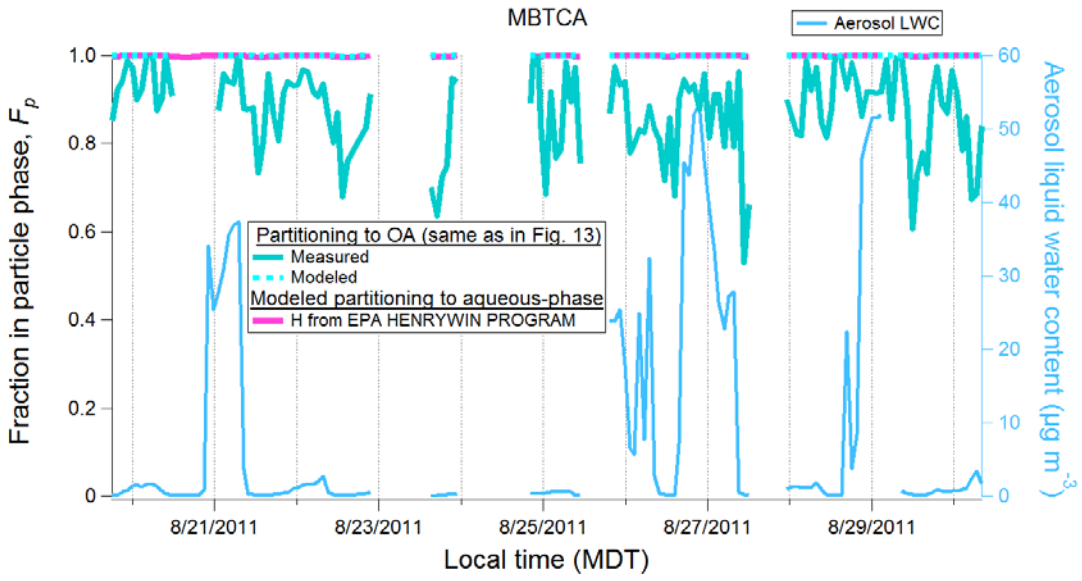

Figure S16. Time series of partitioning to organic and aqueous-phases for 3-methyl-1, 2, 3-butanetricarboxylic acid (MBTCA). Also shown is the time series of ambient temperature and aerosol LWC calculated using the E-AIM model-II.

11. Model simulation of pinic acid with constant ambient temp and constant OA

To investigate the effect of changing ambient temperature and OA on phase partitioning of organic acids we performed two simulations in which we either held the ambient temperature or ambient OA constant in the model. Fig. S17 shows the observed and modeled F_p along with model results when ambient temperature is held constant of 16 ^{o}C and ambient OA is held constant at 2.4 µg m^{-3} and for simplicity, we only show results for pinic acid. The model with changing OA and constant ambient temperature results in much smaller variations in F_p. On the other hand, the model with changing ambient temperature and constant OA shows a pronounced variation in F_p that is more similar to the observed F_p. It is interesting to note the similarity in both the modeled (with changing ambient temperature) and observed F_p when the ambient temperature is highest and with the rapid temperature decrease that follows. These results clearly indicate that temperature is the major driver of phase partitioning at this site.

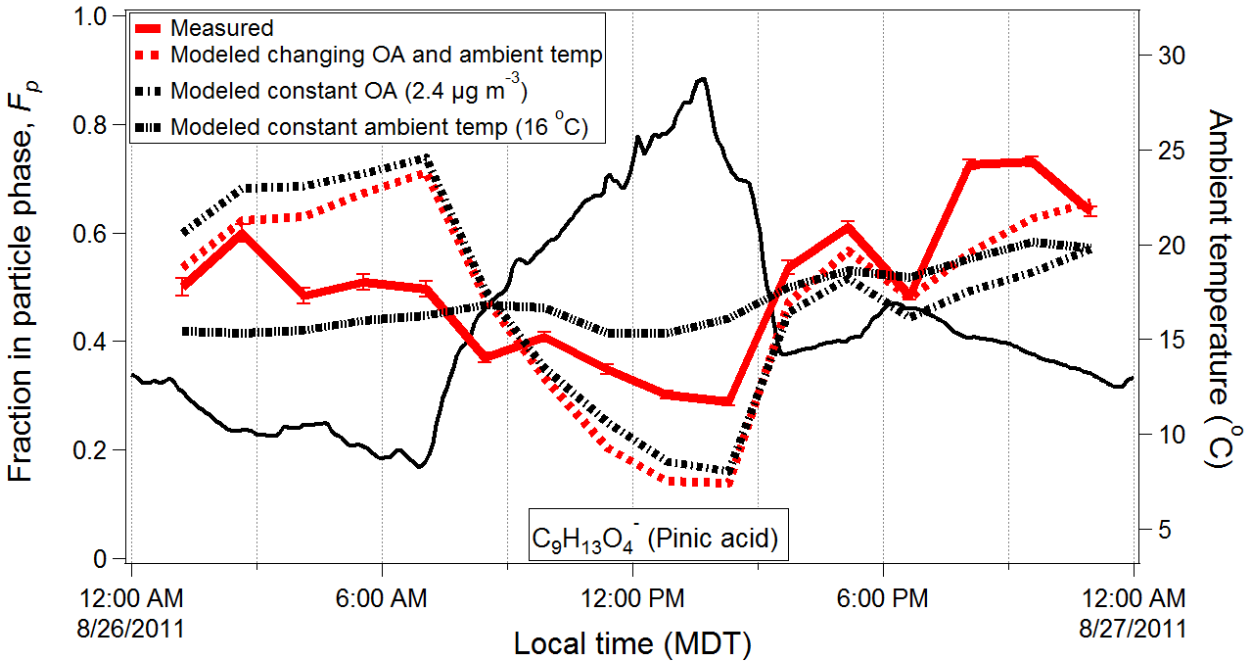

Figure S17. Measured and modeled time series of F_p for pinic acid on August 26, 2011. Model simulations are also shown with (a) changing ambient OA and temperature (b) ambient OA held constant at 2.4 µg m^{-3}, (c) ambient temperature held constant at 16 °C.

Table S1: *VP* and ΔH_{vap} used for phase-partitioning of alkanoic acids. P_v and C^* values are corrected for average ambient temperatures of 289 K on August 26, 2011 from that reported in the literature.

Acid	n_C	P_v (torr)	C^* ($\mu g\ m^{-3}$)	ΔH_{vap} ($kJ\ mol^{-1}$)	Ref
Methanoic	1	25.37	6.4×10^7	46	a
		14.88	3.78×10^7		e
		9.95	2.53×10^7		f
Ethanoic	2	8.66	2.9×10^7	52.3	a
		7.51	2.49×10^7		e
		5.97	1.98×10^7		f
Propanoic	3	2.06	8.4×10^6	57.3	a
		1.86	7.59×10^6		e
		1.67	6.83×10^6		f
Butanoic	4	3.91×10^{-1}	1.9×10^6	63.6	a
		4.83×10^{-1}	2.34×10^6		e
		4.94×10^{-1}	2.4×10^6		f
Pentanoic	5	1.08×10^{-1}	6.0×10^5	62.4	a
		1.4×10^{-1}	7.89×10^5		e
		1.65×10^{-1}	9.26×10^5		f
Hexanoic	6	2.36×10^{-2}	1.5×10^5	73.2	a
		3.8×10^{-2}	2.43×10^5		e
		5.14×10^{-2}	3.29×10^5		f
Heptanoic	7	7.1×10^{-3}	5.1×10^4	72	a
		1.18×10^{-2}	8.41×10^4		e
		1.84×10^{-2}	1.32×10^5		f
Octanoic	8	2.16×10^{-3}	1.7×10^4	82.9	a
		3.37×10^{-3}	2.66×10^4		e
		6.12×10^{-3}	4.85×10^4		f
Nonanoic	9	6.52×10^{-4}	5.7×10^3	85.7	a
		1.05×10^{-3}	9.1×10^3		e
		2.22×10^{-3}	1.93×10^4		f
Decanoic	10	1.87×10^{-4}	1.8×10^3	101.8	b
		3.02×10^{-4}	2.85×10^3		e
		7.5×10^{-4}	7.07×10^3		f
Undecanoic	11	6.75×10^{-5}	6.9×10^2	93.65	a
		1.03×10^{-4}	1.06×10^3		e
		3.03×10^{-4}	3.09×10^3		f
Dodecanoic	12	1.40×10^{-5}	1.5×10^2	111.8	b
		3.04×10^{-5}	3.33×10^2		e
		1.05×10^{-4}	1.14×10^3		f
Tridecanoic	13	3.73×10^{-6}	44	117.65	d
		9.7×10^{-6}	1.14×10^2	78.76	c
		9.72×10^{-6}	1.14×10^2		e
		3.96×10^{-5}	4.63×10^2		f

Acid	n_C	$P^o_{L.i}$ (torr)	C^* (μg m^{-3})	ΔH_{vap} (kJ mol^{-1})	Ref
Tetradecanoic	14	8.38 x 10^{-7}	10	123.5	b
		5.23 x 10^{-6}	65.6	80.5	c
		3.13 x 10^{-6}	39		e
		1.52 x 10^{-5}	1.89 x 10^{2}		f
Pentadecanoic	15	1.63 x 10^{-7}	2.2	131.8	d
		2.02 x 10^{-6}	26.8	102.77	c
		1.0 x 10^{-6}	13.2		e
		5.79 x 10^{-6}	76.5		f
Hexadecanoic	16	3.19 x 10^{-8}	4.5 x 10^{-1}	140.1	b
		9.9 x 10^{-7}	13.9	80.29	c
		3.22 x 10^{-7}	4.59		e
		2.23 x 10^{-6}	31.2		f
Heptadecanoic	17	1.26 x 10^{-8}	1.8 x 10^{-1}	141.6	d
		5.52 x 10^{-7}	8.17	99.65	c
		1.07 x 10^{-7}	1.57		e
		8.93 x 10^{-7}	13.1		f
Octadecanoic	18	4.95 x 10^{-9}	7.7 x 10^{-2}	143.1	b
		2 x 10^{-7}	3.1	97.5	c
		3.54 x 10^{-8}	5.48 x 10^{-1}		e
		3.58 x 10^{-7}	5.55		f

a – Reaxys database (2012), b – Cappa et al. (2008), c – Chattopadhya and Ziemann (2005), d – linear interpolation, e – Nannoolal et al. (2008), f – Marydal and Yalkowsky (1997).

Table S2: P_v, C^* and ΔH_{vap} used for estimating phase partitioning of terpenoic acids. P_v values are for 298 K.

Acid	Elemental Comp	$P^o_{L.i}$ (torr)	C^* (μg m^{-3})	ΔH_{vap} (kJ mol^{-1})	Ref
OH-Glutaric	$C_5H_8O_5$	2.65 x 10^{-8}	2.1 x 10^{-1}	101	b,c
Terpenylic	$C_8H_{12}O_4$	9.75 x 10^{-7}	9.03	42	a
Pinonic	$C_{10}H_{16}O_3$	1.0 x 10^{-4}	1 x 10^{3}	98	d,e
Pinic	$C_9H_{14}O_4$	9.97 x 10^{-7}	10	109	a
OH-Pinonic	$C_{10}H_{16}O_4$	5.7 x 10^{-7}	6.14	122	e,f
MBTCA	$C_8H_{12}O_6$	9.09 x 10^{-11}	1 x 10^{-3}	164	e,g

a – Bilde and Pandis (2001), b – P_v estimated by reducing glutaric acid P_v measured by Bilde and Pandis (2001) by 5.7 x 10^{-3} due to addition of hydroxyl group. c – ΔH_{vap} from Salo et al. (2010) for glutaric acid. d – assumed P_v for pinonic acid similar to Muller et al. (2012). e – ΔH_{vap} estimated using Eq. (12) of Epstein et al. (2010). f - P_v estimated by reducing pinonic acid P_v assumed by Muller et al. (2012) by 5.7 x 10^{-3} due to addition of hydroxyl group. g – assumed P_v for MBTCA similar to Muller et al. (2012).

Table S3: Henry's law constants (M atm^{-1}) used for aqueous partitioning calculations. Mono- and di-acids from EPA HENRYWIN program (2013) are geometric mean values of bond and group-contribution values. H values for multifunctional acids are weighted by excess O as described in section 7 above.

Number of carbons	Mono-acids EPA HENRYWIN Program	Di-acids EPA HENRYWIN Program	Di-acids Compernolle and Müller (2013)	Multifunctional acids Hodzic et al. (2013)
1	1615.32	-	-	-
2	2491.36	4.14938×10^7	1.24599×10^8	52772.1
3	1820.58	2.457×10^8	7.82395×10^9	2.29929×10^6
4	1328.67	6.74743×10^8	1.51344×10^9	4.23578×10^6
5	970.773	4.93015×10^8	1.30565×10^9	1.51086×10^6
6	709.059	3.59924×10^8	1.43004×10^9	1.10739×10^7
7	517.85	2.62812×10^8	2.63975×10^9	3.99458×10^6
8	377.426	1.91685×10^8	7.96501×10^8	1.41546×10^7
9	275.932	1.40243×10^8	5.69497×10^8	2.05538×10^6
10	201.6	1.0243×10^8	2.08433×10^8	
11	147.241	7.47822×10^7		
12	107.469	5.45832×10^7		
13	78.4609	3.98429×10^7		
14	57.2561	2.91566×10^7		
15	41.8428	2.12804×10^7		
16	30.5809	1.55282×10^7		
17	22.3143	1.13351×10^7		
18	16.2889	8.27192×10^6		

REFERENCES

Bilde, M., and Pandis, S. N.: Evaporation rates and vapor pressures of individual aerosol species formed in the atmospheric oxidation of α- and β-pinene, Environ. Sci. Technol., 35, 3344-3349, 2001.

Cappa, C. D., Loverjoy, E. R., and Ravishankara, A. R.: Evaporation rates and vapor pressures of the even-numbered C8-C18 monocarboxylic acids, J. Phys. Chem. A, 112, 3959-3964, 2008.

Chattopadhyay, S., and Ziemann, P. J.: Vapor pressures of substituted and unsubstituted monocarboxylic and dicarboxylic acids measured using an improved thermal desorption particle beam mass spectrometry method, Aerosol Sci. Technol., 39, 1085-1100, 2005.

ChemIDplus Lite - Databases on toxicology, hazardous chemicals, environmental health, and toxic releases (1986), National Library of Medicine (US), Division of Specialized Information Services, Bethesda, MD, USA, Available at http://chem.sis.nlm.nih.gov/chemidplus/chemidlite.jsp, Accessed on July 12, 2012.

Clegg, S. L., Brimblecombe, P., and Wexler, A. S.: A thermodynamic model of the system H^+ - NH_4^+ - SO_4^{2-} - NO_3^- - H_2O at tropospheric temperatures, J. Phys. Chem. A, 102, 2137-2154, 1998.

Compernolle, S., and Muller, J.-F.: Henry's law constants of di-acids and hydroxypolycids: recommended values, Atmos. Chem. Phys. Discuss., 13, 25125-25156, 2013.

E-AIM: Extended aerosol inorganic model II. Available at http://www.aim.env.uea.ac.uk/aim/aim.php. Accessed July 12 2012, 2012.

Estimation Programs Interface Suite™ for Microsoft® Windows, v 4.1 - HENRYWIN v 3.2 (2013), United States Environmental Protection Agency, Washington, DC, USA, Available at http://www.epa.gov/oppt/exposure/pubs/episuite.htm, Accessed on

Epstein, S. A., Riipinen, I., and Donahue, N. M.: A semiempirical correlation between enthalpy of vaporization and saturation concentration for organic aerosol, Environ. Sci. Technol., 44, 743-748, 2010.

Hodzic, A., Madronich, S., Aumont, B., Lee-Taylor, J., Karl, T., Camredon, M., and Mouchel-Vallon, C.: Limited influence of dry deposition of semivolatile organic vapors on secondary organic aerosol formation in the urban plume, Geophys. Res. Lett., 40, doi:10.1002/grl.50611, 2013.

Muller, L., Reinnig, M.-C., Naumann, K. H., Saathoff, H., Mentel, T. F., Donahue, N. M., and Hoffmann, T.: Formation of 3-Methyl-1,2,3-Butanetricarboxyllic acid via gas phase oxidation of pinonic acid - A mass spectrometric study of SOA aging, Atmos. Chem. Phys., 12, 1483-1496, 2012.

Myrdal, P. B., and Yalkowsky, S. H.: Estimating pure component vapor pressures of complex organic molecules, Ind. Eng. Chem. Res., 36, 2494-2499, 1997.

Nannoolal, Y., Rarey, J., and Ramjugernath, D.: Estimation of pure component properties Part 3. estimation of the vapor pressure of non-electrolyte organic compounds via group contributions and group interactions, Fluid Phase Equilibria, 269, 117-133, 2008.

Reaxys database (2012), Reed Elsevier Properties SA, Available at https://www.reaxys.com/reaxys/secured/start.do, Accessed on July 12, 2012.

Salo, K., Jonsson, A. M., Andersson, P. U., and Hallquist, M.: Aerosol volatility and enthalpy of sublimation of carboxylic acids, J. Phys. Chem. A, 114, 4586-4594, 2010.

Sander, R. (2011), "Henry's Law Constants" in NIST chemistry WebBook, NIST standard reference database number 69, edited by P. J. Linstrom and W. G. Mallard, National Institute of Standards and Technology, Gaithersburg, MD.